

# Study on Multi-parameter Mechanical and Microstructural Characteristics of Mining-used Cement-based Grouting Materials

**Xianda Zang**

School of Energy Science and Engineering, Henan Polytechnic University, Jiaozuo 454003, China

Email: 1801157937@qq.com

**How to cite this paper:** Zang, X. D. (2026). Study on Multi-parameter Mechanical and Microstructural Characteristics of Mining-used Cement-based Grouting Materials. *Advances in Engineering Research : Possibilities and Challenges*, 4(2), 1 - 11. ISSN Print: 3079-5192; ISSN Online: 3079-5206.

<https://doi.org/10.63313/AERpc.9098>

**Published: 2026-05-06**

Copyright © 2026 by author(s) and Erytis Publishing Limited.

This work is licensed under the Creative Commons Attribution International License (CC BY 4.0).

<http://creativecommons.org/licenses/by/4.0/>



## Abstract

To investigate the reinforcement effects of two grouting materials, laboratory tests were conducted using ordinary Portland cement and ultra-fine cement as the test materials. Taking the consolidated bodies of cement-based grouts as the research objects, tests on slurry flow characteristics, uniaxial compressive tests on consolidated bodies, and scanning electron microscopy (SEM) tests were carried out to study the mechanical properties of cement-based grout consolidated bodies with different water-cement ratios. The test results show that the viscosity of ordinary cement-based grout decreases with the increase of water-cement ratio, while the bleeding rate increases accordingly. The uniaxial compressive strength of ordinary cement-based consolidated bodies decreased by 35.1%, 43.9% and 5.2% respectively with the increase of water-cement ratio. Meanwhile, the average cumulative acoustic emission ring counts of ordinary cement-based consolidated bodies decreased by 76.7%, 71.1% and 50.1% respectively with the increase of water-cement ratio. Compared with ordinary cement grout at the water-cement ratio of 1:1, ultra-fine cement grout has lower viscosity and bleeding rate, and its consolidated body exhibits higher uniaxial compressive strength and larger cumulative ring counts. Analysis of SEM micrographs reveals that the ultra-fine cement consolidated body has fewer internal defects, more stable structure and stronger bearing capacity. The above test results indicate that ultra-fine cement can achieve significantly better reinforcement performance as a grouting material than ordinary Portland cement.

## Keywords

Portland Cement; Ultra-fine Cementitious Materials; Rheological Characteristics of Grout; Mechanical Properties of Consolidated Bodies; Acoustic Emission; Microstructural Characteristics

## 1. Introduction

In recent years, with the increase in mining depth, deep mining has become a common practice [1-3]. During deep mining, affected by the "three highs and two

disturbances" environment, complex roadway disturbances occur frequently [4,5]. As a common support method, grouting reinforcement can improve the bearing capacity of roadway surrounding rock, enhance the waterproof and impermeability capacity of rock, and improve the overall stability. It has maintained high research popularity and been increasingly widely applied in the support of deep soft rock roadways [6-11].

Domestic and foreign scholars have conducted extensive research on the mechanical properties of consolidated bodies of grouting materials [12-14]. Kang Hongpu and Zhang Zhenfeng [15-16] developed a micro-nano inorganic-organic composite modified material to address the problem that conventional grouting materials cannot penetrate micro-fissures. Through scanning electron microscopy (SEM) observations, they found that the grout can penetrate fissures with a width of 2  $\mu\text{m}$ , the consolidated body is dense and tightly bonded with the coal mass, and the mechanical properties of the bonded coal mass are superior to those of the original coal mass. Zhang Hongwei [17] established a Bingham fluid diffusion-bonding-consolidation (D-Rb-C) coupling model to realize the calculation of the whole process of grout diffusion and consolidation in roadway surrounding rock. They carried out numerical simulation tests of coal-rock mass grouting mechanics using this model and conducted mechanical property tests on the grouted coal-rock mass. Zeng Xiwen [18] used ultra-fine Portland cement as the cementitious material to develop high-performance cement-based grouting materials. Through mechanical bearing capacity tests and acoustic emission (AE) tests, he investigated the influence laws of polypropylene fiber content on the mechanical properties, bleeding property, volume shrinkage property and microstructure of grouting materials. Liu Xuewei [19] selected three grouting materials, namely sulphoaluminate cement, ordinary Portland cement (OPC) and epoxy resin, to reinforce pre-fissured rock samples. They conducted uniaxial compression tests, AE tests and SEM experiments to explore the reinforcement effects of different grouting materials. Wang Yanfang [20] aimed to solve the problems of poor permeability and low early strength of mine-used grouting materials. Based on multiple research methods, they investigated the effects of raw material particle size on the permeability, mechanical properties and microstructure of grouting materials under different water-cement ratios (W/C), and developed an early-strength ultra-fine cement grouting material accordingly.

## **2. Experimental Scheme Design**

### **2.1. Preparation of Cement-based Grout Consolidated Body Specimens**

This experiment aims to analyze the rheological properties, bleeding properties of grouting materials and the strength of cement-based grout consolidated bodies, and investigate the relationship between the mechanical properties of consolidated bodies and water-cement ratio (W/C) as well as their crack development

characteristics.

#### (1) Test Materials

Four groups of ordinary Portland cement (OPC) weighing 1000 g each were weighed using an electronic balance, and four groups of water with volumes of 400 mL, 600 mL, 800 mL and 1000 mL respectively were measured using a measuring cup. The above four groups of cement were added to the corresponding four groups of water respectively and stirred for 5 minutes to prepare ordinary cement-based grouts with W/C ratios of 0.4:1, 0.6:1, 0.8:1 and 1:1. One group of ultra-fine cement (UFC) weighing 1000 g was weighed using an electronic balance, and 1000 mL of water was measured using a measuring cup. The above materials were mixed and stirred for 5 minutes to prepare ultra-fine cement-based grout with a W/C ratio of 1:1.

#### (2) Specimen Preparation

Firstly, considering the size effect, acrylic plates were used to heighten the molds for pouring the three ordinary cement-based grouts with W/C ratios of 0.6:1, 0.8:1, 1:1 and the ultra-fine cement-based grout with a W/C ratio of 1:1. The cement-based grout with a W/C ratio of 0.4:1 is very stable and has no bleeding property, so the triple molds were still used for it. The pouring heights were 100 mm, 102 mm, 112 mm and 124 mm respectively, so that the height of the specimens could be maintained at about 100 mm after solidification, reducing the error caused by the size effect. Five groups of cubic specimens with dimensions of 100×100×100 mm were prepared, with 3 specimens in each group, totaling 15 specimens.



**Figure 1.** Ordinary cement slurry solidified body specimen

## 2.2. Test Equipment and Methods

The RMT-150B rock mechanics test system was used to load the consolidated body specimens of broken mudstone. The test system consists of a loading system, a high-speed camera system and an acoustic emission (AE) system.

A Photron SA1.1200K-M1 high-speed camera was used to record the entire process of the specimens from loading to final failure, and the failure modes of the consolidated body specimens were analyzed.

A DS5-8B full-information acoustic emission signal analysis and test system was used to collect the fracture signals during the uniaxial compression process of the consolidated bodies and analyze their internal fracture conditions.

### 3. Analysis of Fluidity and Bleeding Properties of Cement-based Grouts

#### 3.1. Analysis of Fluidity and Bleeding Properties of Ordinary Portland Cement (OPC) Grouts

##### (1) Relationship between Fluidity (Viscosity) and Water-Cement Ratio (W/C)

Fluidity is a crucial indicator for grouting materials. Good fluidity enables grouting materials to better penetrate into the target grouting areas and achieve superior reinforcement effects. The cement-based grout with a W/C ratio of 0.4:1 had extremely poor fluidity and was almost non-flowable, so the other three groups of cement-based grouts were used for fluidity testing.

The fluidity test was conducted using an MLN-2 Marsh funnel viscometer. The uniformly stirred grout was immediately poured into the vertically placed Marsh funnel. After filling 1500 mL of grout, the time required for the grout to flow down to the 946 mL mark of the grout cup was recorded, which was the Marsh funnel viscosity of the grout in seconds. The results are shown in Figure 2.

As can be seen from Figure 2, when the W/C ratio increased from 0.6:1 to 0.8:1, the viscosity of the grout decreased slightly by only 10.1%, and the grout remained relatively viscous. When the W/C ratio increased from 0.8:1 to 1:1, the viscosity of the grout decreased sharply by 47.2%, indicating that the viscosity of ordinary Portland cement grout decreases with the increase of W/C ratio.

##### (2) Relationship between Bleeding Property and Water-Cement Ratio (W/C)

Bleeding property is one of the key factors reflecting the stability of cement grout. The higher the bleeding rate, the worse the stability of the cement grout. The bleeding rate test was carried out using a 100 mL graduated cylinder.

As shown in Figure 2, the liquid level of the cement-based grout with a W/C ratio of 0.6:1 dropped by 2 mm, that with a W/C ratio of 0.8:1 dropped by 11 mm, and that with a W/C ratio of 1:1 dropped by 20 mm. The bleeding property increased with the increase of W/C ratio. Through calculation, the bleeding rates of the grouts with W/C ratios of 0.6:1, 0.8:1 and 1:1 were 2%, 11% and 20% respectively, indicating that the bleeding property of ordinary Portland cement grout increases with the increase of W/C ratio.

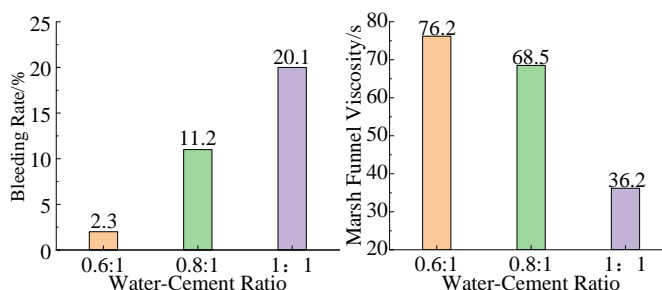


**Figure 2.** Relationship between viscosity, water separability and water-cement ratio of ordinary cement slurries

### 3.2. Fluidity and Bleeding Property of Ultra-fine Cement (UFC) Grouts

#### (1) Relationship between Fluidity (Viscosity) and Water-Cement Ratio (W/C)

The Marsh funnel viscosity data of ultra-fine cement-based grouts with 3‰ naphthalene-based superplasticizer added and W/C ratios of 0.8:1 and 1:1 were selected and compared with those of ordinary cement-based grouts.

At a W/C ratio of 0.8:1, the viscosity of ultra-fine cement grout decreased by 35.2% compared with that of ordinary cement grout; at a W/C ratio of 1:1, the viscosity of ultra-fine cement grout was very close to that of ordinary cement grout, but still decreased by 5.6%. Under the same W/C ratio condition, ultra-fine cement-based grout exhibits better fluidity than ordinary cement-based grout, is easier to inject as a grouting material, and has more advantages in grouting operations.

#### (2) Relationship between Bleeding Property and Water-Cement Ratio (W/C)

The bleeding rate data of ultra-fine cement-based grouts with 3‰ naphthalene-based superplasticizer added and W/C ratios of 0.8:1 and 1:1 were selected and compared with those of ordinary cement-based grouts.

At a W/C ratio of 0.8:1, the bleeding rate of ultra-fine cement grout decreased by 86.3% compared with that of ordinary cement grout; at a W/C ratio of 1:1, the bleeding rate of ultra-fine cement grout decreased by 75% compared with that of ordinary cement grout. The bleeding rate of ordinary cement-based grout is much higher than that of ultra-fine cement-based grout, indicating that ultra-fine cement-based grout exhibits better stability than ordinary cement-based grout, and there is a significant difference in bleeding rate between the two under the same W/C ratio condition.

## 4. Analysis of Stress-Strain Evolution Process of Cement Paste Consolidated Bodies

### 4.1. Stagewise Variation Characteristics of Stress-Strain Curves

The uniaxial compression stress-strain curves of ordinary cement-based consolidated bodies are shown in Figure 3. The stress-strain curves during the uniaxial compression process of consolidated bodies can be roughly divided into four stages: compaction stage, elastic stage, elastoplastic stage and failure stage.

**(1) Compaction Stage:** Due to the dislocation of internal crystals and the closure of pre-existing cracks in the cement-based consolidated body, it enters the compaction stage. The stress-strain curve of the consolidated body is concave upward with a gradually increasing slope, and the consolidated body exhibits nonlinear deformation.

**(2) Elastic Stage:** The axial stress and axial strain increase approximately linearly. The stress increases rapidly while the strain increases slowly, and the slope of the stress-strain curve remains basically unchanged. The consolidated body exhibits elastic deformation.

**(3) Plastic Deformation Stage:** Microcracks begin to appear in the consolidated

body and develop continuously, and the continuous propagation of cracks eventually leads to failure. Rupture occurs after reaching the maximum bearing capacity, and the rapid development of cracks causes the stress of the consolidated body to start decreasing, which lasts for a long time.

**(4) Post-peak Failure Stage:** The internal structure of the consolidated body is basically completely destroyed. Cracks develop rapidly, propagate and coalesce, leading to instability failure of the consolidated body and a rapid decline in bearing capacity. The stress decreases gradually and then plummets, while the strain increases continuously.

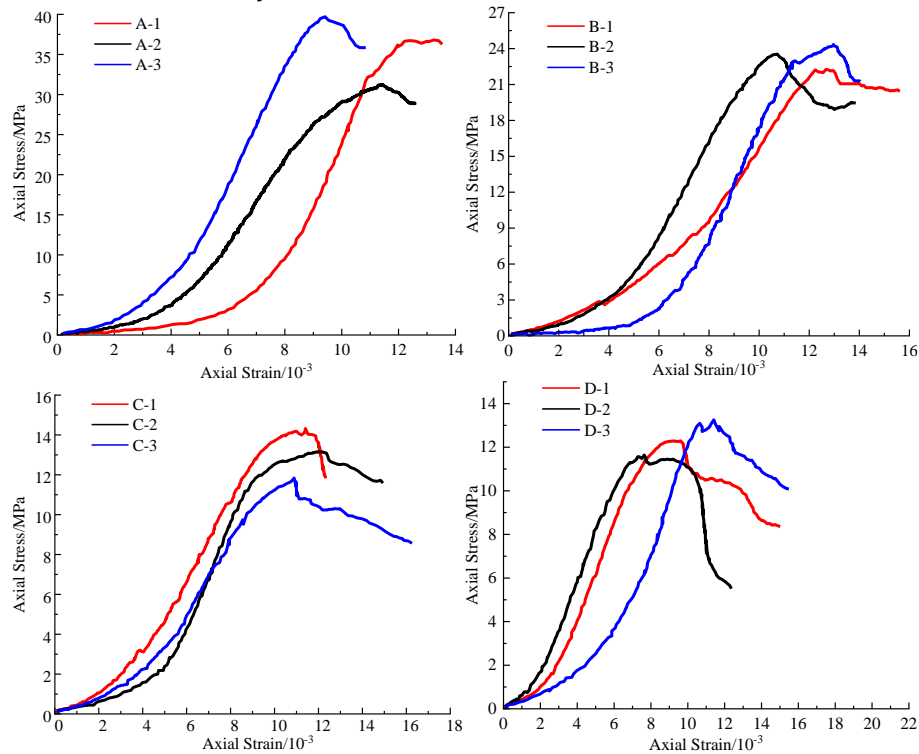


**Figure 3.** uniaxial compression stress-strain curve of consolidated body

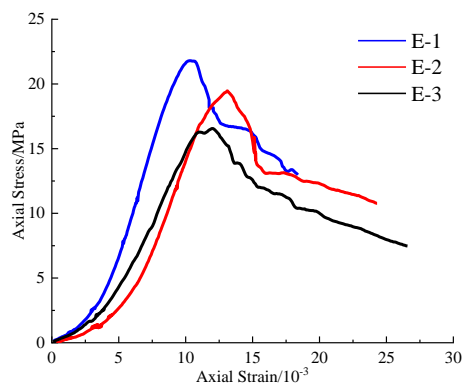


**Figure 4.** superfine cement uniaxial compression stress-strain curve of consolidated body

## 4.2. Relationship between Uniaxial Compressive Strength (UCS) of Ordinary Cement-based Consolidated Bodies and Water-Cement Ratio (W/C)

In accordance with the provisions of the National Standard of the People's Republic of China Standard for Test Methods of Physical and Mechanical Properties of Cement-based Grouts (GB/T 50081-2019), the cubic compressive strength of cement-based grouts shall be calculated according to the following formula:

$$f_{cc} = \frac{F}{A} \quad (1)$$

where:  $f_{cc}$  is the cubic compressive strength of cement-based grout specimens (MPa),  $F$  is the failure load of the specimen (N), and  $A$  is the bearing area of the specimen ( $\text{mm}^2$ ). The uniaxial compressive strength of the consolidated bodies was statistically calculated and plotted according to Equation (1), and the results are shown in Figure 8.

The variation law of the uniaxial compressive strength of ordinary cement-based consolidated bodies is as follows: the uniaxial compressive strength of the consolidated bodies shows an overall gradual decreasing trend with the increase of W/C ratio. When the W/C ratio increased from 0.4:1 to 0.6:1 and 0.8:1, the average uniaxial compressive strength of the consolidated bodies decreased from 36.0 MPa to 23.4 MPa and then to 13.1 MPa, representing decreases of 35.1% and 43.9% respectively. When the W/C ratio increased from 0.8:1 to 1:1, the decreasing trend of uniaxial compressive strength tended to be gentle, with the uniaxial compressive strength decreasing from 13.1 MPa to 12.4 MPa, a reduction of only 5.2%.

## 4.3. Comparison of Uniaxial Compressive Strength (UCS) between Ultra-fine Cement (UFC) and Ordinary Portland Cement (OPC) Consolidated Bodies

Figures 5 show the stress-strain curves of ultra-fine cement-based grout consolidated bodies and ordinary Portland cement-based grout consolidated bodies under uniaxial compression, respectively, both with a W/C ratio of 1:1. It can be seen from the figures that the UCS of ultra-fine cement consolidated bodies is generally higher than that of ordinary Portland cement consolidated bodies, and their loading stroke is also longer. The UCS of group E1, which has the highest strength among the ultra-fine cement consolidated bodies, reaches 21.79 MPa, while that of group D3, the highest strength group among the ordinary Portland cement consolidated bodies, is only 12.31 MPa. The bearing capacity of ultra-fine cement consolidated bodies is almost twice that of ordinary Portland cement consolidated bodies.

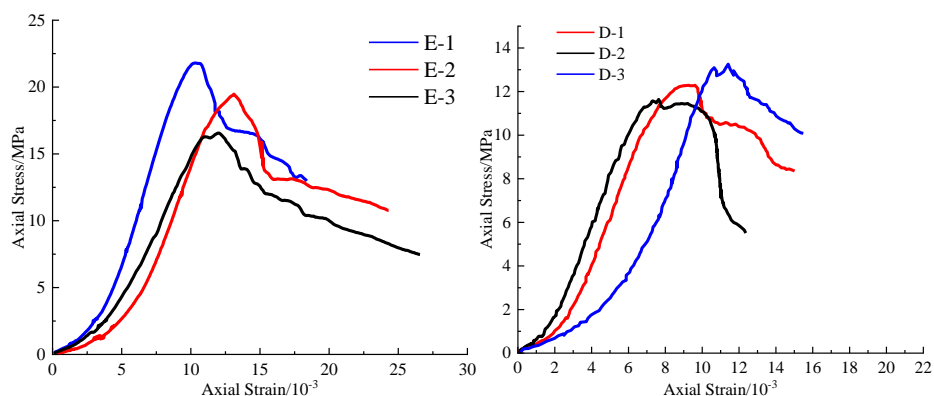


**Figure 5.** uniaxial compression stress-strain curve of superfine cement consolidated body

Through calculation, the average uniaxial compressive strength of the three groups of ultra-fine cement consolidated bodies is 19.26 MPa, and that of the three groups of ordinary Portland cement consolidated bodies is 12.41 MPa, which is 35.6% lower than the strength of ultra-fine cement consolidated bodies, indicating that the strength of ultra-fine cement consolidated bodies is significantly higher than that of ordinary Portland cement consolidated bodies.

## 5. Analysis of Acoustic Emission (AE) Characteristics of Cement-based Consolidated Bodies under Uniaxial Compression

### 5.1. Full-process Analysis of Acoustic Emission

Figure 6 shows the curves of acoustic emission parameters versus time during the whole uniaxial compression process of ordinary cement-based consolidated bodies. Given that ring count and energy are two characteristic parameters of acoustic emission signals, they can reflect the acoustic emission characteristics during the deformation and failure process of consolidated bodies to a certain extent. Therefore, the ring count per unit time, energy, cumulative ring count and cumulative energy were selected as research parameters to analyze the full-process characteristics of acoustic emission.

At a W/C ratio of 0.4:1, a large number of acoustic emission signals were generated in the initial stage of uniaxial compression, which was caused by the dislocation of internal crystals and the closure of pre-existing cracks in the consolidated body. There were three sudden increases in ring count throughout the test, which were speculated to be caused by the propagation and development of main cracks and pre-existing cracks in the consolidated body, leading to a sudden activation of acoustic emission. The ring count reached the maximum at the peak axial stress.

At a W/C ratio of 0.6:1, the number of sudden increase points of ring count in the consolidated body increased, indicating that new cracks and pre-existing cracks developed rapidly under concentrated stress, and the increase of internal defect structures led to a decrease in the bearing capacity of the consolidated body.

At a W/C ratio of 0.8:1, an obvious excitation stage appeared in the acoustic emission signals of the consolidated body. Before the axial stress reached the peak, two sudden increase points of ring count appeared, and the ring count was evenly distributed in other stages, indicating that at least two main cracks had developed and formed at these two time points until they propagated through and destroyed the entire consolidated body.

At a W/C ratio of 0.4:1, the acoustic emission ring counts were evenly distributed before and after the peak axial stress, and were in the excitation stage at the peak axial stress. The development and formation of main cracks generated a large number of signals, resulting in a sharp increase in ring count.

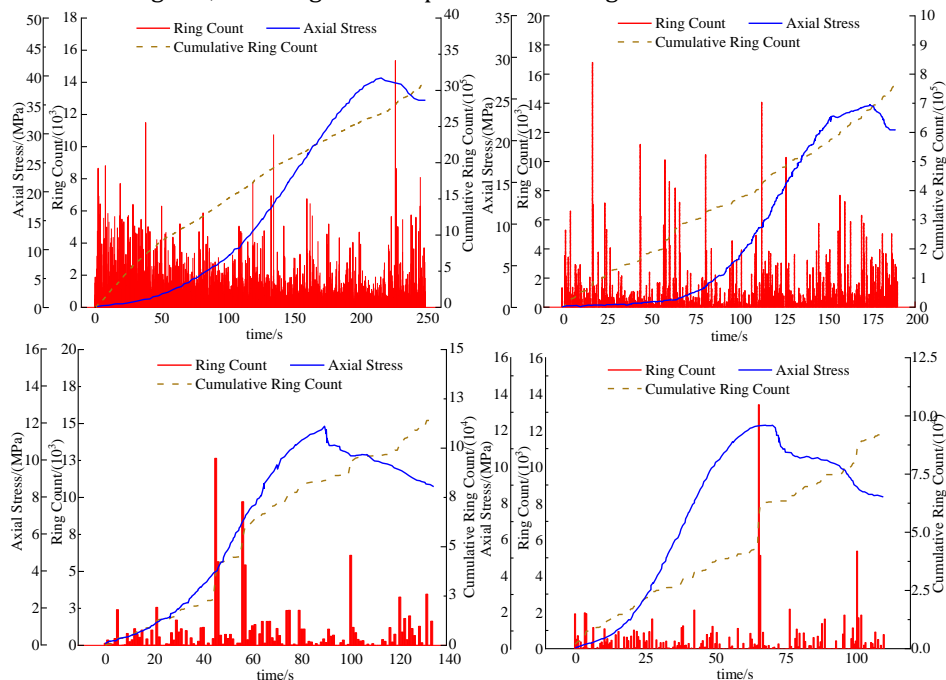


Figure 6. acoustic emission ringing count of junction under uniaxial compression

### 5.2. Relationship between Acoustic Emission (AE) Characteristics and Water-Cement Ratio (W/C)

To ensure the reliability of the data, outliers with excessive dispersion in the statistical data were eliminated and the remaining data were plotted. The variation law of ring counts during the uniaxial compression process of consolidated bodies is as follows: the average cumulative ring count of cement-based grout consolidated bodies shows a decreasing trend with the increase of W/C ratio. When the W/C ratio increased from 0.4:1 to 0.6:1, the cumulative ring count decreased by 76.7%; when the W/C ratio increased from 0.6:1 to 0.8:1, the cumulative ring count decreased by 71.1%; when the W/C ratio increased from 0.8:1 to 1:1, the cumulative ring count decreased by 50.1%.

Through the above comparative analysis, it can be concluded that the average

cumulative ring count of the consolidated body with a W/C ratio of 0.4:1 is the highest among all consolidated bodies, followed by that with a W/C ratio of 0.6:1. At a W/C ratio of 0.4:1, the grout has the highest density and the consolidated body exhibits the maximum strength. At a W/C ratio of 1:1, the grout has the lowest density and the consolidated body shows the poorest strength.

## 6. Conclusions

- (1) The viscosity of ordinary Portland cement (OPC) grout decreases with the increase of water-cement ratio (W/C), while the water bleeding rate increases with the increase of W/C. Both the viscosity and water bleeding rate of ultra-fine cement (UFC) grout are lower than those of OPC grout.
- (2) The uniaxial compressive strength (UCS) of OPC-based consolidated bodies decreases with the increase of W/C ratio. With the increase of W/C ratio, the average UCS of consolidated bodies decreased by 35.1%, 43.9% and 5.2% sequentially from 36.0 MPa to 12.4 MPa. At a W/C ratio of 1:1, the average strength of UFC-based consolidated bodies is 19.26 MPa, which is 55.3% higher than that of OPC-based consolidated bodies.
- (3) Compared with OPC, UFC-based grout has lower viscosity and lower water bleeding rate at the same W/C ratio, making it easier to inject and more stable. UFC-based consolidated bodies have higher strength at the same W/C ratio. This indicates that ultra-fine cement has better performance as a grouting material and can produce better reinforcement effect after grouting.

## References

- [1] He M. C., Xie H. P., Peng S. P., et al. Study on Rock Mechanics in Deep Mining[J]. Chinese Journal of Rock Mechanics and Engineering, 2005, 16: 2803-2813.
- [2] Jiang P. F., Kang H. P., Wang Z. G., et al. Principle, Technology and Application of Bolt-Frame-Filling Collaborative Control for Surrounding Rock of Soft Rock Roadway in Kilometer Deep Mine[J]. Journal of China Coal Society, 2020, 45(3): 1020-1035.
- [3] Kang Y. S., Liu Q. S., Liu B., et al. Exploration on Step-by-Step Combined Support Technology of Precise Intervention in Surrounding Rock Structure of Deep Rock Roadway[J]. Chinese Journal of Rock Mechanics and Engineering, 2023, 42(11): 2682-2693.
- [4] Hou C. J. Effective Approach for Surrounding Rock Control of Deep Roadways[J]. Journal of China University of Mining & Technology, 2017, 46(3): 467-473.
- [5] Lan H., Chen D. K., Mao D. B.. Analysis on Current Situation of Deep Coal Mining and Disaster Prevention in China[J]. Coal Science and Technology, 2016, 44(1): 39-46.
- [6] Tang Y. Application of Grouting Technology in Surrounding Rock Reinforcement and Support of Deep Roadways[J]. Coal Technology, 2021, 40(11): 50-53.
- [7] Zhou H., Wang X., Liu H., et al. Effect analysis of grouting reinforcement ring considering fluid solid coupling[J]. MATEC Web of Conferences, 2019, 277: 3014.
- [8] Li Z., Li S., Liu H., et al. Experimental Study on the Reinforcement Mechanism of Segmented Split Grouting in a Soft Filling Medium[J]. Processes, 2018, 6(8): 131.
- [9] Wang H. B., Zheng Q. S., Liu R. T., et al. Grouting reinforcement mechanism and experimental study of cement quick-setting slurry infiltration[J]. IOP Conference Series: Earth and Environmental Science, 2017, 81(1).

- 
- [10] Kang H. P., Feng Z. Q. Current Situation and Development Trend of Grouting Reinforcement Technology for Surrounding Rock of Coal Mine Roadways[J]. *Coal Mining Technology*, 2013, 18(3): 1-7.
- [11] Zhang Y., Wang S., Zhang B., et al. A preliminary investigation of the properties of potassium magnesium phosphate cement-based grouts mixed with fly ash, water glass and bentonite[J]. *Construction and Building Materials*, 2020, 237: 117501.
- [12] Lu H. F., Zhu C. D., Liu Q. S. Study on Shear Mechanical Properties of Structural Planes under the Action of Different Grouting Materials[J]. *Chinese Journal of Rock Mechanics and Engineering*, 2021, 40(9): 1803-1811.
- [13] Liu R. T., Zheng Z., Li S. C., et al. Study on Mechanical Properties of Broken Rock Mass after Grouting Reinforcement[J]. *China Journal of Highway and Transport*, 2018, 31(10): 284-291.
- [14] Rong M. R. Study on Mechanical Properties and Failure Mechanism of Grouting Reinforced Body in Surrounding Rock Fractures[D]. Shijiazhuang Tiedao University, 2020.
- [15] Kang H. P., Jiang P. F., Huang B. X., et al. Collaborative Control Technology of Support-Modification-Pressure Relief for Surrounding Rock of Roadways in Kilometer Deep Coal Mines[J]. *Journal of China Coal Society*, 2020, 45(3): 845-864.
- [16] Zhang Z. F., Kang H. P., Jiang Z. Y., et al. Development and Practice of High-Pressure Split Grouting Modification Technology for Roadways in Kilometer Deep Mines[J]. *Journal of China Coal Society*, 2020, 45(3): 972-981.
- [17] Zhang H. W., Jiang H., Liu S. Q., et al. Mechanism and Law of Grouting Reinforcement in Broken Rock Mass Based on D-Rb-C Coupling Model[J]. *Journal of China Coal Society*, 2023, 48(4): 1464-1475.
- [18] Zeng X. W., Wang Y. F., Zhao G. M., et al. Study on Properties of Polypropylene Fiber Modified Ultra-Fine Cement Composite Grouting Material[J]. *Coal Science and Technology*, 2024, 52(7): 57-67.
- [19] Liu X. W., Wang S., Liu B., et al. Study on Mechanical Properties of Rock-Like Specimens with Double Fractures Filled with Different Grouting Materials[J]. *Chinese Journal of Rock Mechanics and Engineering*, 2024, 43(3): 623-638.
- [20] Wang Y. F., Ai J., Cheng X., et al. Effect of Ultra-Fine Processing on Microstructure and Mechanical Properties of Sulfoaluminate Cement Grouting Materials under High Water-Cement Ratio[J/OL]. *Coal Science and Technology*, 1-13[2024-12-26].